30th NENE 2021
September 6 - 9
BLED-SLOVENIA
International Conference Nuclear Energy for New Europe

Kinetic-Fluid Coupling Time-Dependent Simulations Of ITER During ELMs

Ivona Vasileska[1], **Xavier Bonnin** [2], **Leon Kos** [1]
[1] Faculty of Mechanical Engineering, University of Ljubljana
Aškerčeva 6, 1000 Ljubljana, Slovenia
ivona.vasileska@lecad.fs.uni-lj.si
leon.kos@lecad.fs.uni-lj.si

[2] ITER Organization
Route de Vinon-sur-Verdon - CS 90 046 - 13067 St Paul Lez Durance Cedex - France
xavier.bonnin@iter.org

ABSTRACT

Edge Localized Modes (ELMs)-induced transient heat loads on the divertor targets represent a important threat to target lifetime and can lead to the need to replace them with a frequency that has a major impact in the execution of the ITER Research Plan. Predicting the impact of such large transient heat loads through modelling is especially challenging and is often attempted through the use of fluid plasma boundary modelling codes, such as SOLPS-ITER, in which the ELM is crudely approximated as a fixed large, but limited in time, increase in anomalous cross-field transport coefficients for particles and heat to mimic a specified total ELM energy loss. However, one problem with this approach is that the boundary conditions at the target sheath interface are expected to vary strongly in time through the ELM transient. The kinetic heat flux limiters are fixed and typically applied in the fluid codes. Coupling kinetic fluid codes has not yet been systematically used for ITER ELMs study.

This contribution describes the first results of efforts to address ELMs issues for ITER simulations under high performance conditions using the 1D3V (1D in space and 3D in velocity) electrostatic parallel Particle-in-Cell (PIC) code BIT1 [1], to study the kinetic effects and to provide time dependent kinetic target sheath heat transmission factors (SHTF). In a later stage of the work, these will be used in the formulation of fluid boundary conditions for calculations of ELM target heat loads using the SOLPS-ITER code.

The BIT1-SOLPS-ITER coupling allows us to investigate the kinetic effects on the targets, by comparing power and particle fluxes from time-dependent simulations of ITER Type I ELMs.

1 INTRODUCTION

The preferred operation regime for current and future tokamak reactors, such as ITER, is the high confinement H-mode. However, H-modes are often subject to plasma relaxation events, known as Edge Localised Modes (ELMs), during which a large transient heat load to the divertor may occur [2, 3, 4]. The ELMs cause a sudden drop in plasma pressure at the edge of the confined region, leading to a significant loss of plasma energy. The lost plasma energy is carried by parallel transport in the scrape-off layer (SOL) [5] to the divertor plates.

In current tokamaks the energy flux through the SOL during ELMs is several MJm^{-2}, but in next-generation tokamaks, such as ITER, it is expected to be much larger [6, 7, 8], i.e. several tens of MWm^{-2}, all deposited onto the targets in a matter of milliseconds. Such violent events can pose a serious threat to the long-term resistance of the divertor materials [7, 9] .

The SOL is one of the most complex regions of the plasma, where a lot of physical and chemical processes take place. Also, the SOL is a mediator between the hot core plasma and the solid surfaces, for that reason, it should be accurately modelled [10].

While modelling SOL plasmas, different numerical models are used, depending on the physical aspect [11]. The most complete description is to provide a kinetic theory, which accounts for the motion of each particle in the plasma. The whole kinetic description for the plasma at the microscopic level can be written using the well-known Boltzmann equation and Maxwell equations [5, 12]. But, at the macroscopic level, the plasma is described using a fluid model. The main focus of the fluid model is to represent the external plasma parameters, which are functions of time and position. In fluid models the core plasma can be modelled as a one-fluid model using the MHD set of equations [13].

However, the fluid model for the SOL is not self-contained; it requires kinetic flux limiters as well as boundary conditions (BCs) inside the sheath region that come from external models [1]. The goal of the present study is to investigate ELMs to obtain the relevant boundary parameters, namely the sheath heat-transmission factors, and insert them in the fluid code.

As a kinetic tool for calculating the sheath's heat-transmission factors, the PIC/MC code BIT1[14] was used. These results are already presented in the articles [15, 16, 17]. The coefficients in this work will be used as boundary parameters in the plasma fluid code SOLPS-ITER [18, 19].

2 FLUID MODELLING

The SOLPS-ITER package is a sophisticated code suite intended for edge plasma modelling and divertor design studies. In this work, the SOLPS-ITER code was modified to use the obtained boundary parameters from BIT1, as a constant during the pre-ELM phase, than at different times along the Type-I ELM duration and after ELM (post-ELM) phase. The code modifications are explained in the SOLPS-ITER manual.

The SHTF (sheath heat transmission factors) investigated here appear as [1, 20, 21]:

1. Boundary conditions for the ion parallel speed and particle energy fluxes at the plasma sheath entrance

$$M = \frac{V_{\parallel}^{i}}{C_s}; \quad \gamma^{e,i} = \frac{Q_{sh}^{e,i}}{\Gamma^{e,i} \cdot T^{e,i}}; \quad \varphi = \frac{e\Delta\phi}{T^{e}}; \tag{1}$$

2. Particle heat flux and ion viscosity expressions used in fluid codes

$$q_{\parallel} = \left(\frac{1}{q_{SH}} + \frac{1}{aq_{FS}}\right)^{-1} \pi_{\parallel} = \left(\frac{1}{\pi_{\parallel}^{Br}} + \frac{1}{bnT}\right)^{-1}; \tag{2}$$

where M is Mach number, $C_s = \sqrt{\frac{Te+\delta_i T_i}{m_i}}$ is the ion-sound speed, $\gamma^{e,i}$ are the electron and ion sheath heat transmission factor, $\Gamma^{e,i}$ are the electron and ion fluxes to the divertor and φ is the normalized potential drop, respectively. $m_{e,i}$ and $T_{e,i}$ are electron and ion masses and electron and ion temperature. Here δ_i (~ 1)is the polytrophic constant. $q_{SH} = -\chi_{\parallel}\partial_s T$ and

$q_{FS} = \Gamma T$ are the Spitzer-Harm and the free-streaming heat fluxes, and $\pi_{\parallel}^{Br} = -\frac{4}{3}\eta_{\parallel}\partial_s V_{\parallel}$ is the Braginskii ion parallel viscosity term. The SHTF represent the Mach number M , the sheath heat transmission coefficients γ, the normalized potential drop φ and the heat and viscosity limiters, a and b.

The SHTF obtained from BIT1, during ELM-free at 200 μs, Type-I ELM at 400 μs and post-ELM at 200 μs, using the Eqs. 1 and 2 are presented in the following Table.1.

Table 1: SHTF obtained from BIT1 during all ELM phases

SHTF	ELM-free	Type-I ELM	Post-ELM
M	1	2	1
$\gamma_{e,wall}$	2	3	2
$\gamma_{i,wall}$	7	6.5	7
$\gamma_{e,sheath}$	4	5	4
$\gamma_{i,sheath}$	4	7	4
a_e	0.1	0.3	0.1
a_i	0.1	0.5	0.1
b	0.5	1	0.5

The first step in this exercise was to establish a "steady state" (stable plasma in which plasma parameters do not change over time) without SHTF. Next was simulate the whole ELM cycle, first the pre-ELM (ELM-free) phase which corresponds to the "steady state" but with SHTF, second Type-I ELM which corresponds to the time over which MHD activity is high or interval over recycling emission or power flux rise, and third post-ELM, which corresponds to the time of relaxation. For each ELM cycle the SHTF given in Table 1 were used.

The burning plasma conditions correspond to the ITER Q = 10, 15 MA baseline at q_{95} = 3, assuming typical upstream separatrix parameters of n_e ∼3 to 5 · 10^{19} m^3, $T_e \sim$ 100 to 150 eV and $T_i \sim$ 200 to 300 eV.

To check if this method for BIT1-SOLPS-ITER coupling is correct, JET simulations on BIT1 were done and after validation of the results the JET SHTF values were used in SOLPS-ITER.

The obtained results were compared against similar simulations (kinetic and fluid coupling) done in the articles [22, 9]. From the comparison, we conclude that this method, adding the SHTF from BIT1 into SOLPS-ITER, which can be used in the case of ITER. In this work, ITER low power case with D-fuelled was used, and the plasma particles, electrons, ions (D^+), neutrals (D) and molecules (D_2) were simulated.

3 RESULTS AND DISCUSSION

For the time-dependent ELMs simulations, we chose $dt = 10^{-7}$ time steps, providing 2000 points, covering a total of 400 μs. The time-dependent results (at the separatrix, which is a boundary between domains with distinct dynamical behaviour (phase curves) in a dynamical system) of n_e, T_e, T_i and Φ_{tot} at the inner and outer divertors during all the ELMs phases are presented in Fig. 1.

From time evolution profiles at the divertor targets, the plasma parameters during ELM-free phase are constant, because this phase correspond to the steady-state. When ELM starts from 100 to 300 μs T_e, T_i and ϕ increases up, for T_e till 12 eV and 23 eV, T_i up to 12 eV and 18 eV and ϕ till 20 V and 31 V at the inner and outer divertors, respectively. The particle

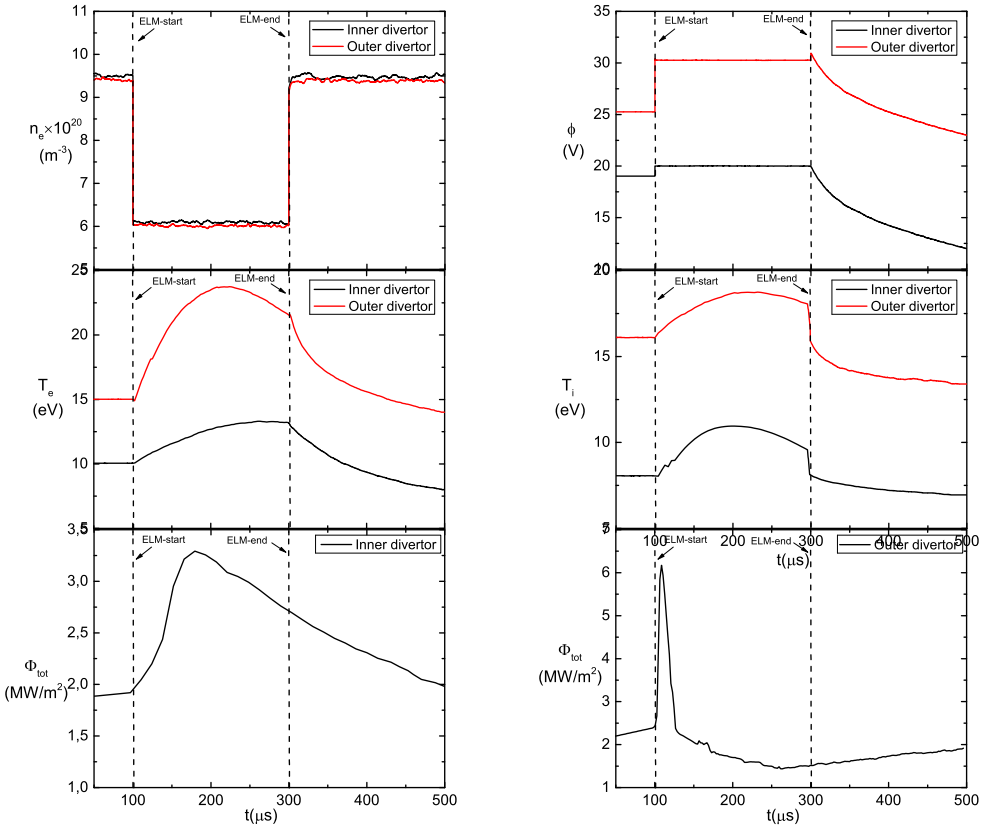

Figure 1: ITER time-dependent n_e, T_e, T_i and Φ_{tot} profiles at inner (left) and (outer) right divertors during ELMs

temperatures also increases during ELM due to the energy and recycling that affect on the electrons and ions respectively. This influence is greater at the outer divertor accordingly to the heat transfer from inner to outer divertor during ELM. The plasma potential is not changed during ELM time, so the ELM does not affect on it. n_e has different tendency. When the ELM starts n_e decreases to 6×10^{20} m^{-3}. The ITER plasma during ELM has strong recycling for that reason, the density is lower during ELM. The total energy flux increases up to 3.25 MW/m^2 at 180 μs at inner and 6 MW/m^2 at 110 μs at outer divertor, due to the sudden drop at the pedestal. At inner divertor during ELM decreases slightly, but at the outer divertor the energy flux decreases suddenly. This shows that, the total flux energy at the outer divertor when ELM stars increases, reach the maximum, and after that decrease slowly due to the slow energy reduction during the ELM. But, at outer divertor the energy during ELM decreases suddenly due to the fast recombination. For that reason, is very important to control the heat flux at outer divertor because this abrupt change can destroy the divertor. In this case using the boundary conditions obtained from the BIT1 control, to keep this changes in the frame between 3-6 MW/m^2. After ELM when relaxation time starts, post-ELM phase, all plasma parameters, expect plasma density, decreases reaching the values which were before ELM, so the plasma tends to be back at the steady state.

The time-dependent results for electron temperature (T_e), ion temperature (T_i), electron density(n_e) and plasma potential (ϕ) at the midplane during Type-I ELM (from the other graphs is obviously that during ELM-free the values will be constant and during post-ELM they will tend to have the same values as the ELM-free) are presented at Fig. 2.

From the upstream profiles during Type-I ELM T_e is slightly decreasing from 111 to 107

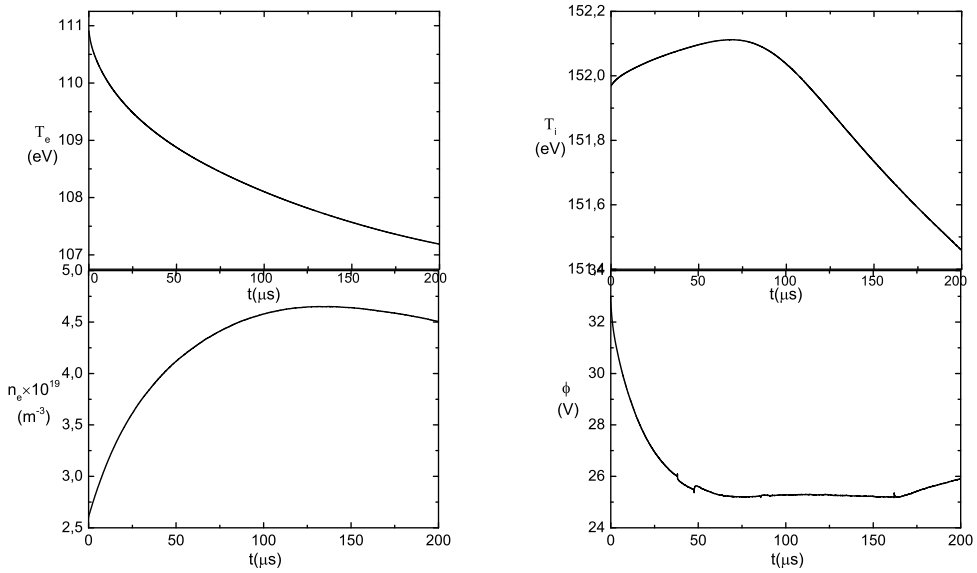

Figure 2: ITER time-dependent T_e, T_i, n_e and ϕ profiles at the midplane during Type-I ELM

eV, but the T_i increases at 70 μs to 151 eV and then is decreasing to 151.4 eV. These tendencies show that during ELM the heat energy is decreasing, but the recycling is maximum at 70 μs. Also the prove that the recycling is maximum at 70 μs, is shown at the n_e profile. Density increases till 70 μs and then it remains constant. The plasma potential has the maximum value at the moment when the ELM starts, 33 V and then is decreasing until the ELM crash due to the energy consumption.

To sum up, during ELM-free the plasma parameters are not changed due to the plasma steady state. When ELM starts, the ITER plasma has strong recycling and for that reason, the density has lower values. The temperatures, potential and total energy fluxes increases due to the heat energy that occur in the plasma. At the midplane, the recycling is the strongest at 70 μs, but the heat energy is decreasing until the ELM crash. After ELM the values tend to be equal as were in ELM-free phase or steady state.

4 CONCLUSION

In this work, the kinetic code BIT1 and the fluid code SOLPS-ITER were coupled. The SHTF obtained from BIT1 were introduced into the SOLPS-ITER code as a boundary conditions. With the changes done in the SOLPS-ITER code the right positions, where the flux limiters should be applied to control the heat loads at the targets can now be defined. In this work, we showed that if the initial profiles do not have sharp gradients in the near-core area, an ELM can have little impact on the target profiles, in spite of the work done in [8]. After this initial proof-of-principle attempt, more realistic studies will require core profiles with higher plasma pressure inside the separatrix, which will cause larger heat fluxes to flow towards the targets shown in [7].

Over time, from target profiles due to the strong recycling in the ITER plasma during ELM the density decreases. The power energy affects on the particle temperatures, total heat flux and potential. The total flux energy at the outer divertor when ELM stars increases, reach the maximum, and after that decrease slowly due to the slow energy reduction during the ELM. But, at outer divertor the energy during ELM decreases suddenly due to the fast recombination.

For, that reason is very important to control the heat flux at outer divertor because this abrupt change can destroy the divertor. At midplane the heat energy during time is decreasing, bu the recycling increases.

ACKNOWLEDGMENTS

The simulations were performed at the ITER HPC cluster. The views and opinions expressed herein do not necessarily reflect those of the ITER Organisation.

REFERENCES

[1] D. Tskhakaya, F. Subba, X. Bonnin, D. P. Coster, W. Fundamenski, and R. A. Pitts. On kinetic effects during parallel transport in the SOL. *Contribution Plasma Phys*, 48(1-3):335–338, March 2008.

[2] J. W. Connor. Edge-localized modesphysics and theory. *Plasma Physics and Controled Fusion*, 40(5):531542, January 1998.

[3] J. W. Connor, A. Kirk, and H. R. Wilson. Edge localised modes (ELMs): Experiments and theory. *AIP Conference Proceedings*, 1013(1):174, May 2008.

[4] A. S. Kukushkin, H. D. Pacher, V. Kotov, G. W. Pacher, and D. Reiter. Finalizing the ITER divertor design: The key role of SOLPS modeling. *Fusion Engineering and Design*, 86(12):2865–2873, December 2011.

[5] Peter Stangeby. Analytic expressions for shaping analysis of the ITER outer wall. *Nuclear Fusion*, 51(10):103015, 2011.

[6] T. H. Osborne, K. H. Burrell, R. J. Groebner, L. L Lao, A. W. Leonard, R. Maingi, R. L. Miller, G. D. Porter, G. M. Staebler, and A. D. Turnbull. H – mode pedestal characteristics in ITER shape discharges on DIII-D. *Journal of Nuclear Materials*, 266-269:131–137, March 1999.

[7] R.A. Pitts, X. Bonnin, F. Escourbiac, H. Frerichs, J.P. Gunn, T. Hirai, A.S. Kukushkin, E. Kaveeva, M.A. Miller, D. Moulton, V. Rozhansky, I. Senichenkov, E. Sytova, O. Schmitz, P.C. Stangeby, G. De Temmerman, I. Veselova, and S. Wiesen. Physics basis for the first iter tungsten divertor. *Nuclear Materials and Energy*, 20:100696, 2019.

[8] T. Eich, B. Sieglin, A.J. Thornton, M. Faitsch, A. Kirk, A. Herrmann, and W. Suttrop. ELM divertor peak energy fluence scaling to ITER with data from JET, MAST and ASDEX upgrade. *Nuclear Materials and Energy*, 12:84 – 90, 2017.

[9] D. M. Harting, S. Wiesen, M. Groth, S. Brezinsek, G. Corrigan, G. Arnoux, P. Boerner, S. Devaux, J. Flanagan, A. Jarvinen, S. Marsen, D. Reiter, and JET-EFDA contributors. Intra-ELM phase modelling of a JET ITER-like wall H-mode discharge with EDGE2D-EIRENE. *Journal of Nuclear Materials*, 463:493–497, August 2015.

[10] S. Wiesen, M. Groth, M. Wischmeier, S. Brezinsek, A. Jarvinen, F. Reimold, and L. Aho-Mantila. Plasma edge and plasma-wall interaction modelling: Lessons learned from metallic devices. *Nuclear Materials and Energy*, 12:3 – 17, 2017.

[11] Gianpiero Colonna and Antonio DAngola. *Plasma Modeling*. IOP Publishing, Bristol, 2016.

[12] W. B. Thompson. *Introduction to Kinetic Theory of Plasma*. Springer, Boston, MA, 1st ed. edition, 1968.

[13] S. I. Braginskii. *Transport Processes in a Plasma*. Consultants Bureau, New York, 1965.

[14] D. Tskhakaya. One-dimensional plasma sheath model in front of the divertor plates. 59(11401):19pp, 2017.

[15] I. Vasileska, D. Tskhakaya, and L.Kos. Time-dependent boundary conditions during Type-I ELM in ITER scrape-off-layer. In *28th Int. Conf. Nuclear Energy for New Europe*, pages 709.1–709.8, Portorož, Slovenia, 09-12 Sept. 2019.

[16] I. Vasileska, D. Tskhakaya, and L.Kos. Time-dependent kinetic factors in ITER scrape-off-layer. In *29th Int. Conf. Nuclear Energy for New Europe*, pages 709.1–709.8, Portorož, Slovenia, 09-12 Sept. 2020.

[17] I.Vasileska and L. Kos. Time-dependent boundary conditions during ELMs in ITER plasma. *Journal of Fusion Energy*, 39:212–220, March 2020.

[18] X. Bonnin, W. Dekeyser, R.A. Pitts, D. Coster, S. Voskoboynikov, and S. Wiesen. Presentation of the new SOLPS-ITER code package for tokamak plasma edge modelling. *Plasma Fusion Research*, 11:1403102, August 2016.

[19] S. Wiesen, D. Reiter, V. Kotov, M. Baelmans, W. Dekeyser, A. S. Kukushkin, S. W. Lisgo, R. A. Pitts, V. Rozhansky, G. Saibene, I. Veselova, and S. Voskoboynikov. The new SOLPS-ITER code package. *Jounral of Nuclear Materials*, 463:480–484, August 2015.

[20] D. Tskhakaya, S. Kuhn, and Y. Tomita. Formulation of boundary conditions for the unmagnetized multi-ion-component plasma sheath. *Contrib. Plasma Phys.*, 46(7-9):640–654, 2006.

[21] W. Fundamenski. Parallel heat flux limits in the tokamak scrape-off layer. *Plasma Physics and Controlled Fusion*, 47(11):R163R208, July 2005.

[22] R. A. Pitts, P. Andrew, G. Arnoux, T. Eich, W. Fundamenski, A. Huber, C. Silva, D. Tskhakaya, and JET EFDA Contributors. ELM transport in the JET scrape-off layer. *Nuclear Fusion*, 47(11):14371448, October 2007.